

科技关注

硫酸盐三价铬镀液中次磷酸钠浓度对不锈钢阳极电化学溶出的抑制作用

蒋义锋, 杨防祖, 许书楷, 田中群, 周绍民

(厦门大学化学化工学院化学系 固体表面物理化学国家重点实验室, 福建 厦门 361005)

[摘要] 为了进一步完善以316不锈钢为阳极的硫酸盐三价铬镀铬新工艺, 考察了镀液中次磷酸钠等对316不锈钢阳极电化学溶出的抑制作用。利用Hull槽试验、能量射散谱(EDS)和扫描电子显微镜(SEM)研究了次磷酸钠浓度对镀层外观、组分和表面形貌的影响。结果表明, 次磷酸钠可以有效地抑制316不锈钢阳极的电化学溶出: 当其浓度为0.020 mol/L时, 316不锈钢阳极的电化学溶出量由无次磷酸钠时的116.7 mg/(A·h)下降到13.1 mg/(A·h); 浓度低于0.040 mol/L时, Hull试样外观没有变化; 浓度低于0.060 mol/L时, 镀层表面形貌无明显变化; 镀层中含磷量随次磷酸钠浓度的提高而逐渐增加。

[关键词] 三价铬镀铬; 次磷酸钠; 抑制剂; 硫酸盐; 不锈钢阳极; 电化学溶出

[中图分类号] TQ153.1; O646

[文献标识码] A

[文章编号] 1001-1560(2011)04-0001-03

0 前言

铬镀层外观优美、硬度高、耐蚀和耐磨性好, 已广泛用作装饰性镀层和功能性镀层^[1,2]。六价铬对环境有严重的危害, 六价铬电镀将被淘汰。为此, 三价铬电镀得到了广泛的研究^[3~5]。目前, 三价铬镀铬体系主要有氯化物、硫酸盐及其混合型3类^[6~8]。三价铬镀铬工艺采用的不溶性阳极包括石墨、钛涂氧化铱(DSA)、铁氧体和隔离阳极。其中, 石墨和DSA阳极使用最广。电镀过程中, 氯化物体系阳极表面易产生氯气, 具有腐蚀性和刺激性, 硫酸盐体系及硫酸盐和氯化物混合体系便成了研究重点。然而, 硫酸盐三价铬镀铬存在许多问题, 如镀液稳定性和抗杂质能力差; 三价铬容易在阳极氧化成六价铬^[9], 直流电镀难以镀厚^[10]; DSA阳极价格昂贵、制作复杂、导电性差^[11,12]等。

已开发的新型硫酸盐三价铬电镀工艺具有许多优点, 且使用不锈钢为阳极^[13~15]。但是, 在施镀时不锈

钢阳极会发生电化学溶出, 溶出的Fe进入镀液。尽管少量的铁离子可以提高镀液的分散能力和镀层的抗腐蚀能力, 但随着电镀时间的延长(电量增加), 镀液中的铁离子杂质将不断增多, 进而影响镀层的组成和抗腐蚀能力。目前, 对不锈钢阳极电化学溶出抑制剂的研究未见报道。

本工作试图用合适的抑制剂减缓不锈钢阳极电化学的溶出, 并研究其对镀层外观、组成和表面形貌的影响。

1 试验

1.1 镀液组成与工艺条件

镀液组成: 以 $\text{Cr}_2(\text{SO}_4)_3 \cdot 6\text{H}_2\text{O}$ 为主盐, 提供 $\text{Cr}(\text{III})$, 浓度0.150 mol/L; $\text{Na}_2\text{C}_2\text{O}_4$ 和 $\text{H}_2\text{C}_2\text{O}_4 \cdot 2\text{H}_2\text{O}$ 为配位剂, 浓度分别为0.120, 0.080 mol/L; H_3BO_3 为缓冲剂, 浓度为0.700 mol/L; Na_2SO_4 为导电盐, 浓度为0.850 mol/L; 添加剂为聚醇、聚醚类有机化合物和含硫有机物的混合物, 浓度为12 000~16 000 m/l。镀液采用化学纯试剂与去离子水配制。

工艺条件: 温度40℃, pH值3.5~4.0, 采用85-Z型恒温磁力搅拌器轻微搅拌; 阴极电流密度4~6 A/dm²; 阳极为316不锈钢, 阴极为抛光黄铜片(约含40%Zn)、镀镍片或紫铜片, 阳极阴极面积比为2:1;

[收稿日期] 2010-10-30

[基金项目] 福建省产业技术开发项目(闽发改高技[2010]299号); 国家自然科学基金项目(20873114); 福建省科技计划重点项目(2008H0086)

[通信作者] 杨防祖, 副教授, 电话: 0592-2185957, E-mail: fzyang@xmu.edu.cn

Hull槽 250 mL, 电流 3 A。

1.2 检测分析

采用 CH I-660 电化学工作站完成电化学测试, 三电极体系: 参比电极为饱和甘汞电极 (SCE), 辅助电极为铂片, 研究电极为 316 不锈钢, 面积为 0.0314 cm², 温度为 25 °C; 从开路电势阳极方向扫描至 +1.45 V, 扫描速率为 100 mV/s。

利用正置金相显微镜 (MX-6R) 观察腐蚀和电化学溶出前后 316 不锈钢表面形貌的变化。利用扫描电子显微镜 (SEM-4800) 和能量射散谱 (EDS) 对镀层进行表征。

2 结果与讨论

2.1 316 不锈钢阳极在镀液中的腐蚀与电化学溶出

316 不锈钢阳极面积为 1 dm², 在 500 mL 镀液中浸渍 3 h 后无腐蚀溶出, 电量为 3 (A·h) 时, 电化学溶出量为 350.1 mg 相当于理论溶出量 3 133.7 mg (Fe²⁺) 的 11.2%, 相应的表面形貌见图 1。从图 1 可知: 316 不锈钢阳极表面腐蚀 3 h 后没有明显的变化, 但电化学溶出后的表面较腐蚀前的粗糙, 并出现一些腐蚀坑。这表明 316 不锈钢阳极不发生腐蚀, 电镀过程中的溶解是由电化学溶出造成的。

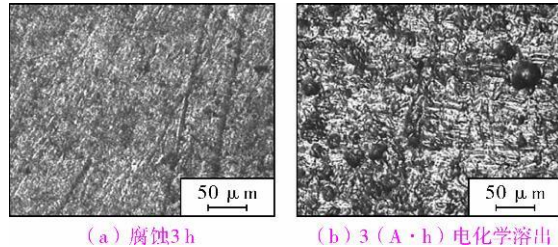


图 1 316 不锈钢阳极腐蚀及电化学溶出后的表面形貌

2.2 还原性物质对 316 不锈钢阳极电化学溶出的影响

理论上讲, 三价铬镀铬液中加入还原性物质对三价铬电镀没有影响; 在电镀过程中, 还原性物质优先在不锈钢阳极发生电化学氧化 (或提高不锈钢阳极溶出的极化作用), 可以抑制不锈钢的阳极溶出。不同还原性物质对 316 不锈钢阳极电化学溶出的影响见表 1。由表 1 可以看出, 电量为 3 (A·h) 时, 无还原性物质镀液中 316 不锈钢阳极溶出量 (减重) 为 350.1 mg 加入还原性物质, 除次磷酸钠以外, 溶出量减少不明显; 加入 0.100 mol/L 次磷酸钠, 316 不锈钢阳极仅减重 16.7 mg。这一结果表明次磷酸钠对 316 不锈钢阳极的电化学溶出具有明显的抑制作用。

表 1 不同还原性物质对 316 不锈钢阳极电化学溶出的影响 (电量 3 A·h)

还原性物质	C / (mol L ⁻¹)	m (阳极溶出) / mg	还原性物质	C / (mol L ⁻¹)	m (阳极溶出) / mg
-	-	350.1	甲醛	0.100	350.5
亚硫酸钠	0.100	223.1	亚硝酸钠	0.100	321.2
次磷酸钠	0.100	16.7	盐酸羟胺	0.100	312.1
尿素	0.100	292.4	硫脲	0.100	291.4

不含及含有 0.100 mol/L 次磷酸钠镀液中 316 不锈钢阳极的极化曲线见图 2。无次磷酸钠时 316 不锈钢阳极在 0.80 V 左右出现起波氧化电流, 这归因于其电化学的溶出, 随着电势的逐渐正移, 氧化电流逐渐增大, 并于 1.36 V 附近开始析氧; 在含有 0.100 mol/L 次磷酸钠的镀液中, 316 不锈钢阳极在 0.70 V 附近出现起波氧化电流, 且比不含时显著增大, 减重仅为 16.7 mg。这证明 316 不锈钢阳极氧化电流主要归因于次磷酸根的阳极氧化或次磷酸根作用下草酸根的阳极氧化。次磷酸钠比铁的标准电极电势更负 [$E^0(\text{PO}_2^{3-}/\text{PO}_3^{3-}) = -0.499 \text{ V}$, $E^0(\text{H}_3\text{PO}_3/\text{H}_3\text{PO}_4) = -0.276 \text{ V}$, $E^0(\text{Fe}/\text{Fe}^{3+}) = -0.037 \text{ V}$, $E^0(\text{Fe}/\text{Fe}^{2+}) = -0.447 \text{ V}$], 优先在 316 不锈钢阳极表面氧化, 减缓了其氧化溶出。

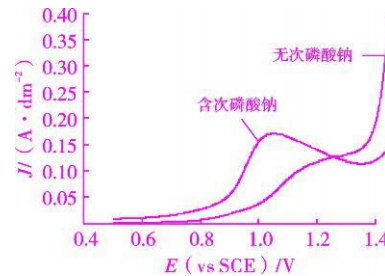


图 2 2 种镀液中 316 不锈钢阳极的极化曲线

2.3 次磷酸钠浓度对 316 不锈钢阳极电化学溶出的影响

镀液中不同次磷酸钠浓度对 316 不锈钢阳极电化学溶出量的影响见图 3。由图 3 可见: 镀液加入 0.005, 0.010, 0.020 mol/L 次磷酸钠后, 316 不锈钢阳极的溶出量分别从不含次磷酸钠时的 350.1 mg 迅速降至 218.7, 91.5, 39.3 mg。次磷酸钠浓度从 0.040 mol/L 增加到 0.100 mol/L 时, 316 不锈钢阳极溶出量均在 20.0 mg 左右。这进一步表明, 次磷酸钠浓度达到 0.020 mol/L 即可以有效抑制 316 不锈钢阳极电化学的溶出, 其溶出量为 13.1 mg/(A·h), 仅为理论值的 1.24%。在硫酸盐三价铬镀铬过程中, 镀液中少量的铁离子对镀液的分散能力有很好的促进作用; 镀液中的铁也与铬发生共沉积。因此, 镀液中加入次磷酸钠后, 316 不

锈钢阳极溶出少量的铁形成的铁离子不会造成累积。

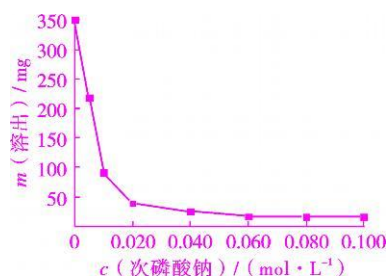


图3 不同次磷酸钠浓度对316不锈钢阳极电化学溶出的影响(电量3 A·h)

2.4 次磷酸钠浓度对镀层外观的影响

不同次磷酸钠浓度对镀层质量的影响见图4。当其浓度低于0.020 mol/L时, 镀层外观无明显变化; 而浓度为0.040 mol/L时, 低端1.5 cm镀层发暗, 浓度继续升高, 发暗区逐渐变宽; 浓度为0.100 mol/L时, 低端6.5 cm均为发暗镀层。以上结果表明, 次磷酸钠浓度为0.020 mol/L时, 镀层外观没有变化, 316不锈钢阳极的电化学溶出量很低。



图4 不同次磷酸钠浓度对镀层外观的影响
△—无镀层 □—暗镀层 ▨—光亮镀层

2.5 次磷酸钠浓度对镀层组分和表面形貌的影响

次磷酸钠浓度对镀层组分的影响见表2。由表2可知: 镀层的主要成分为Cr, 并含有少量的Fe和S。Fe来源于镀液中少量铁离子的共沉积, S来源于电活性添加剂的吸附和夹杂; 基础液中加入次磷酸钠之后, 镀层含有P, 并随着次磷酸钠浓度的提高而逐渐提高; 当次磷酸钠含量为0.020 mol/L时, Fe含量达到极大值。

表2 不同次磷酸钠浓度对镀层组分的影响 %

c/(mol L⁻¹)	w(Cr)	w(Fe)	w(S)	w(P)
0	89.32	7.85	2.83	-
0.005	85.25	8.02	3.14	1.25
0.010	86.83	7.63	3.56	1.98
0.020	85.31	8.32	4.01	2.36
0.040	86.20	6.98	3.23	3.59
0.060	83.11	7.69	2.88	6.32
0.080	78.84	7.58	2.79	10.79
0.100	79.59	5.86	2.56	14.55

图5是次磷酸钠浓度对镀层形貌的影响。由图5可知: 镀液中加入不同浓度的次磷酸钠, 其镀层表面都有细小的颗粒, 并伴有少量针孔; 次磷酸钠浓度低于0.040 mol/L时, 镀层形貌无明显变化; 次磷酸钠浓度达到0.060 mol/L时, 镀层表面开始出现少量较大的颗粒, 并随其浓度的提高, 颗粒数量逐渐增加。

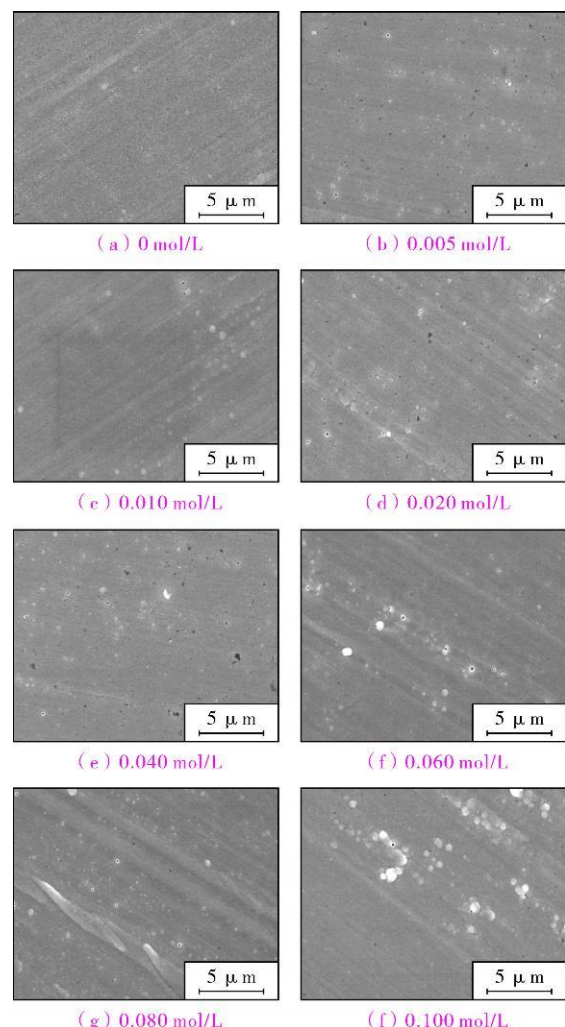


图5 不同次磷酸钠浓度对镀层表面形貌的影响

3 结论

(1) 316不锈钢阳极在硫酸盐三价铬镀铬液中不产生腐蚀, 但在电镀过程中会发生电化学溶出。

(2) 次磷酸钠对316不锈钢阳极的电化学溶出有强烈的抑制作用。其含量为0.020 mol/L时, 镀层外观无变化, 316不锈钢阳极的溶出量也很低, 仅为13.1 mg/(A·h)。

(3) 镀液中加入次磷酸钠, 镀层中会夹杂有少量的磷, 且随其浓度的增加而逐渐提高。

(下转第63页)

提高了Ni-P合金镀层的耐蚀性。Ni-Fe-P镀层具有更好的耐蚀性的原因可以归结为：镀液中加入FeSO₄以后，镀层结晶更加细致、光滑致密，缺陷数量更少，镀层的表面质量得到改善，有助于减少腐蚀介质渗入到基体的通道数量，增大了腐蚀反应阻力所致。

3 结 论

Ni-Fe-P镀层的晶粒比Ni-P合金镀层中的更加细小、致密，表面缺陷数量更少，镀层质量得到改善；膜电阻得到了提高，减少了腐蚀介质渗入到基体的腐蚀通道，增大了在3.5%NaCl溶液中腐蚀时的电荷转移阻力，其耐蚀性比Ni-P镀层高。

[参考文献]

- [1] Babu G V, Palanizppa M, Jayalakshmi M, et al. Electroless Ni-P coated on graphite as catalyst for the electro-oxidation of dextrose in alkali solution [J]. Journal of Solid State

Electrochemistry, 2007, 11(12): 1705~1712.

- [2] AbdelHameed R M, El-Khatib K M. Ni-P and Ni-Cu-P modified carbon catalysts for methanol electro-oxidation in KOH solution [J]. International Journal of Hydrogen Energy, 2010, 35(6): 2517~2529.
- [3] Liu W J, Hsieh S H, Chen W J, et al. Growth behavior of electroless Ni-Co-P deposits on Fe [J]. Applied Surface Science, 2009, 255(6): 3880~3883.
- [4] Baharaju J N, Rajam K S. Electroless deposition and characterization of high phosphorus Ni-P-SiN₄ composite coatings [J]. International Journal of Electrochemical Science, 2007, 2(10): 747~761.
- [5] 孙春文, 唐致远, 郭鹤桐, 等. 化学镀Ni-Co-P合金对M_m(NiCoAlMn)₅贮氢合金电极动力学性能的影响 [J]. 中国稀土学报, 2001, 19(2): 115~120.
- [6] 梁平, 史艳华. 碘酸钾对Q235钢Ni-P化学镀层的影响 [J]. 材料保护, 2010, 43(1): 28~30.

[编校:魏兆军]

(上接第3页)

[参考文献]

- [1] Vykhotseva L N, Edigaryan A A, Lubnin E N, et al. Composition, structure, and corrosion-electrochemical properties of chromium coatings deposited from chromium (III) electrolytes containing formic acid and its derivatives [J]. Russian Journal of Electrochemistry, 2004, 40(4): 387~393.
- [2] Zeng Z X, Sun Y L, Zhang J Y. Tribological and electrochemical behavior of thick Cr-C alloy coatings electrodeposited in trivalent chromium bath as an alternative to conventional Cr coatings [J]. Electrochimica Acta, 2006, 52(3): 1366~1373.
- [3] 胡耀红, 刘建平, 陈力格, 等. 硫酸盐三价铬镀铬工艺 [J]. 电镀与涂饰, 2006, 25(1): 43~45.
- [4] 管勇, 毛祖国, 丁运虎, 等. 硫酸盐体系三价铬电镀工艺研究 [J]. 材料保护, 2007, 40(6): 26~29, 79.
- [5] 赵坤, 孙化松, 李永彦, 等. 硫酸盐电镀三价铬镀层性能研究 [J]. 表面技术, 2009, 38(2): 22~24.
- [6] Zeng Z X, Sun Y L, Zhang J Y. The electrochemical reduction mechanism of trivalent chromium in the presence of formic acid [J]. Electrochemistry Communications, 2009, 11(2): 331~334.
- [7] 胡晓赟, 屠振密, 李永彦, 等. 氯化物三价铬电镀液中六

价铬的去除方法及效果 [J]. 材料保护, 2009, 42(2): 74~76.

- [8] Lee J Y, Kim M, Kwon S C. Effect of polyethylene glycol on electrochemically deposited trivalent chromium layers [J]. Transaction Nonferrous Metals Society of China, 2009, 19(4): 819~823.
- [9] Edigaryan A A, Safnov V A, Lubnin E N, et al. Properties and preparation of amorphous chromium carbide electropolates [J]. Electrochimica Acta, 2002, 47(17): 2775~2786.
- [10] Song Y B, Chin D T. Pulse plating of hard chromium from trivalent baths [J]. Plating and Surface Finishing, 2000, 87(9): 80~87.
- [11] Li B S, Lin A, Wu X, et al. Electrodeposition and characterization of Fe-Cr-P amorphous alloys from trivalent chromium sulfate electrolyte [J]. Journal of Alloys and Compounds, 2008, 453(1/2): 93~101.
- [12] 胡耀红, 陈力格, 赵国鹏, 等. 三价铬镀铬阳极的研究 [J]. 材料保护, 2006, 39(4): 26~28.
- [13] 蒋义锋, 杨防祖, 许书楷, 等. 新型硫酸盐三价铬镀铬工艺 [J]. 材料保护, 2010, 43(8): 32~35.
- [14] 杨防祖, 蒋义锋, 许书楷, 等. 一种硫酸盐三价铬电镀液与制备方法: 中国, 101665960A [P]. 2010-03-10.
- [15] 杨防祖, 蒋义锋, 许书楷, 等. 硫酸盐三价铬镀铬阳极: 中国, 101665974A [P]. 2010-03-10.

[编校:徐军]



Journal of Materials Protection

(Monthly Started in 1960)

ISSN 1001-1560 Apr 2011 Vol 44 No 4 Serial No 387

Contents & Abstracts

Inhibition Effect of Sodium Hypophosphate on Electrochemical Stripping of Stainless Steel Anode in Trivalent Chromium Sulfate Plating Bath

JIANG Yifeng YANG Fangzhi XU Shukai TIAN Zhongqun ZHOU Shaomin (State Key Laboratory of Physical Chemistry of the Solid Surfaces Department of Chemistry College of Chemistry and Chemical Engineering Xiamen University Xiamen 361005 China). *Cailiao Baohu* 2011, 44(04), 01~03(Ch). The inhibition function of sodium hypophosphate for electrochemical stripping of 316 stainless steel anode in trivalent chromium sulfate plating bath was investigated by highlighting the effects of concentration of sodium hypophosphate on the appearance, composition and surface morphology of the coatings based on Hull cell test, energy dispersive spectrometry and scanning electron microscopy. Results show that sodium hypophosphate can effectively inhibit the anodic electrochemical stripping of 316 stainless steel. The introduction of 0.020 mol/L sodium hypophosphate led to the decrease of anodic stripping amount from 116.7 mg/(A·h) to 13.1 mg/(A·h). The appearance of Hull cell panel kept unchanged at a sodium hypophosphate concentration of 0.040 mol/L and below. The surface morphology of the coating also kept unchanged as the concentration of sodium hypophosphate was lower than 0.060 mol/L. The content of phosphorus in the coating increased with increasing concentration of sodium hypophosphate.

Key words: trivalent chromium plating; sodium hypophosphate; inhibitor; sulfate; stainless steel anode; electrochemical stripping

Electrochemical Corrosion Behavior of Electroplated Zinc-Magnesium Alloy Coating in Sodium Chloride Solution

XIN Sen-sen, LI Mou-cheng (Institute of Materials, Shanghai University, Shanghai 210072, China). *Cailiao Baohu* 2011, 44(04), 04~06(Ch). Zn-Mg alloy coating was prepared from a sulfate bath containing octadecyl dimethylbenzyl ammonium chloride and polyethylene glycol additives. The electrochemical corrosion behavior of resultant Zn-Mg alloy coating in 3.5% NaCl solution was investigated by means of scanning electron microscopy, X-ray diffraction and electrochemical impedance spectroscopy. Results indicate that Zn-Mg alloy coating containing 0.35% Mg can be prepared in the presence of synergistic effect of the two types of additives. In the early stage of corrosion, Mg led to relatively low corrosion potential and electrochemical impedance of the alloy coating. However, with extending corrosion duration, Mg was progressively consumed and protective film of the corroded products was instantly formed on the surface of the Zn-Mg alloy coating, resulting in significantly increased corrosion potential and impedance as well as better corrosion resistance.

Key words: Zn-Mg alloy coating; corrosion; sodium chloride solution; electrochemical impedance spectroscopy

Galvanic Corrosion Behavior of Micro-Arc Oxidation Coating on TC4 Titanium Alloy Coupled with Metals

ZHAO Qing ZHU Wen-hui WANG Shuai-xing NING Zheng (National Defense Key Discipline Laboratory of Light Alloy Processing Science and Technology, Nanchang Hangkong University, Nanchang 330063, China). *Cailiao Baohu* 2011, 44(04), 07~10(Ch). Porous ceramic coatings composed of Al_2TiO_5 , anatase TiO_2 and mullite TiO_2 were prepared on the surface of TC4 alloy by micro-arc oxidation. The galvanic corrosion behavior of TC4 alloy and its micro-arc oxidation coating coupled with 45 steel LY12 aluminum alloy and red copper was investigated. It was found that when coupled with TC4 alloy, 45 steel and LY12 experienced serious galvanic corrosion and uneven pitting respectively, but red cop-

per did not show obvious corrosion. Couple current for 45 steel LY12 aluminum alloy and red copper coupled with the TC4 alloy after micro-arc oxidation was reduced to 1/8, 1/11 and 1/3 of that for them metals coupled with untreated TC4 alloy respectively. The galvanic corrosion of TC4 alloy and its coupled metals could be effectively reduced by micro-arc oxidation treatment of the TC4 alloy.

Key words: micro-arc oxidation; titanium alloy; metal couple; galvanic corrosion behavior

Effect of 3-Mercapto-1-Propane Sulfonate Sodium Salt Composite Additive on Electrodeposition of Copper

GU Min¹, ZHONG Qiru² (1 State and Local Joint Engineering Laboratory of Methane Damage in Complex Coal Gas Seam, College of Resources and Environmental Science, Chongqing University, Chongqing 400044, China; 2 Chongqing Chang'an Suzuki Automobiles Company Ltd., Chongqing 401321, China). *Cailiao Baohu* 2011, 44(04), 11~14(Ch). Effect of 3-mercaptopropanesulfonate (MPS) coupled with polypropylene glycol (PEG) and/or CT at different concentrations on copper electrodeposition in acidic copper sulfate bath was investigated by measuring polarization curves and electrochemical impedance spectra (EIS). Measurement results of polarization curves and EIS indicate that a synergistic effect exists between MPS and PEG or CT. MPS-PEG inhibited the electrodeposition of copper, while MPS-CT and MPS-PEG-CT accelerated copper electrodeposition. MPS could generate an intermediate via reaction with CT and $\text{Cu}^{+}/\text{Cu}^{2+}$ under a relatively low potential, and resultant intermediate was adsorbed on the surface of the electrode. MPS inhibited copper electrodeposition but could coordinate with CT, contributing to the acceleration of superconformal filling of copper.

Key words: MPS; PEG; CT; filling of copper; electrodeposition

Microwave Absorbing Performance of Electroless Co-Ni-P Alloy Coating on Fly Ash Hollow Microspheres

ZUO Jincheng^{1,2}, JIANG Jinghua², MA Ai-bin², WANG Zehua², LIN Pinghua² (1 Jiangxi Xingcheng Special Steel Company Ltd., Jiangxi 314429, China; 2 College of Materials Science and Engineering, Hohai University, Nanjing 210098, China). *Cailiao Baohu* 2011, 44(04), 15~18(Ch). A novel lightweight microwave absorbing powder material with core-shell structure was prepared by conducting electromagnetic modification of fly-ash microspheres (5 μm scale) via electroless plating of Co-Ni-P. The effects of electroless plating parameters on the morphology, composition and microwave absorbing performance of Co-Ni-P alloy coating were investigated by using a scanning electron microscope, an energy dispersive spectrometer and a microwave vector network analyzer. Results show that the coating on the surface of cenosphere particles consists of stacked Co-Ni-P spheres with a size of 0.5~1.0 μm . The coating was even in terms of thickness, but its composition was much different from that of the plating bath. Besides, the coated hollow microspheres were magnetic loss dielectric media and possessed strong soft ferromagnetic properties. The coating obtained from the plating bath with a $\text{Co}^{2+}/\text{Ni}^{2+}$ mass ratio of 3:1 had a Co/N mass ratio of 1.34 and the best microwave absorbing performance. When the concentration of hypophosphate in the plating bath was increased to 50 g/L, resultant coating had increased content of amorphous phase and turned into two-phase soft magnetic material showing enhanced microwave absorbing ability. Namely, it had a lowest reflectivity of -31.5 dB, and its frequency range corresponding to a reflectivity below -10.0 dB was as much as 4.5 GHz (8.2~12.7 GHz).